Analytical solution for nonlinear hydrologic routing with general power-law storage function

Behzad Nazari[1] and Dong-Jun Seo[2]

[1]Dept of Civil Eng, The Univ of Texas at Arlington, Box 19308, Rm 247 Nedderman Hall, 416 Yates St., Arlington, TX 76019-0308 (corresponding author). Email: behzad.nazari@mavs.uta.edu

[2]Dept of Civil Eng, The Univ of Texas at Arlington, Box 19308, Rm 248 E Nedderman Hall, 416 Yates St., Arlington, TX 76019-0308. Email: djseo@uta.edu

1. Introduction

Hydraulic routing involves solving the governing equations of conservation of mass and momentum, widely known as the Saint-Venant (S-V) equations (Chanson, 2004). Whereas hydraulic routing models represent the most accurate method for flood routing in theory (Kim and Georgakakos, 2014), they require large amounts of data to prescribe the fixed boundary conditions of channel geometry and elaborate numerical integration to ensure stability and accuracy(Szymkiewicz, 2010). Hydrologic routing models, on the other hand, are significantly simpler and easier to use but can only provide predictions at a limited number of locations due to their lumped nature (Kim and Georgakakos, 2014; Mazzoleni et al., 2018; McCuen, 2004; Noh et al., 2018). Depending on the flow type, accuracy requirement, data availability, and computing power, different hydrologic routing models may be used. Kim and Georgakakos (2014) provided a historical review of hydrologic routing models, including the reservoir routing(Goodrich, 1931), Muskingum (McCarthy, 1938), Lag and K (Linsley et al., 1949), and Muskingum-Cunge (Cunge, 1969), and introduced a new conceptual river routing method based on nonlinear cascade of reservoirs. Storage-based routing models are among the oldest and most widely used in hydrology, including engineering hydrology and operational flood forecasting (Fread and Hsu, 1993; Nourani et al., 2009). The recently launched National Water Model (NWS, 2021a) also uses Muskingum-Cunge as one of the channel routing methods and level pool routing for reservoirs and lakes. As such, advancing hydrologic routing continues to be a significant topic of research. The purpose of this paper is to present new analytical exact and semi-analytical approximate solutions and their applications for nonlinear reservoir routing with general power-law storage where the underlying level pool assumption is justified (see Ayalew et al., 2014; Bentura and Michel, 1997; Chi et al., 2015; Gupta, 2004; Gupta and Waymire, 1998; Mandapaka

Venkata, 2009; Mantilla et al., 2006; Mantilla and Gupta, 2005; Menabde and Sivapalan, 2001; Reggiani et al., 2001; Small et al., 2013 just to name several).

The concept of nonlinear storage in routing is well known. Though the wide channel simplification of the Manning's equation (Orlandini and Rosso, 1998; Yu and Lim, 2003) and the level pool assumption remain controversial (Fread et al., 1978; Goodell and Wahlin, 2009), nonlinear hydrologic routing has been used extensively in hydrologic modeling and prediction, ranging from routing flow through a channel or a storage structure to simulating flow through networks of channels as in CUENCAS (Mantilla and Gupta, 2005) and TOPKAPI (Todini and Ciarapica, 2001). In what follows, a brief background on nonlinear routing with power-law storage as it pertains to the development of this paper is presented. The continuity equation for storage routing is given by (Carter and Godfrey, 1960):

$$\frac{dS}{dt} = I - Q \qquad (1)$$

where I, Q, and S denote the inflow, outflow and storage at time t, respectively. In most real-world applications, the storage and outflow are not known jointly and hence an additional equation is needed to solve Eq. (1). This closing equation relates storage with discharge and is referred to as the storage-outflow relationship, or storage function (Chow et al., 1988; Sugiyama et al., 1997). Numerous studies (Basha, 2000, 1995, 1994; Boyd et al., 1979; Sugiyama et al., 1997; Tallaksen, 1995 to name a few) have postulated that the storage-outflow relationship may be expressed as the following power-law function:

$$S = \kappa Q^{\varepsilon} \qquad (2)$$

where κ and ε denote the storage coefficient and exponent, respectively. In Eq. (2), the assumptions that the storage function is time-invariant or "uniformly nonlinear" (Dooge, 2005), and that S is a proper function of Q are implicitly considered. In Eq. (2), the coefficient κ

measures the ratio between the capacity of the reservoir and that of the discharge from the reservoir. The coefficient κ is larger for a large storage capacity with small outflow and smaller for a small reservoir with large outflow. If an outlet is so large that it is not restricting flow at all, κ is effectively zero (Mitchell, 1962). For $\varepsilon \neq 1$, Eq. (1) becomes nonlinear reservoir routing. The value of ε determines the relative shape of the outflow hydrograph and generally ranges between 0 and 1 with an average of 0.5 for unconfined aquifers (Hammond and Han, 2006). Mitchell (1962) suggested that the lower bound of ε is about 0.67 which corresponds to the critical depth of a reservoir with vertical side walls. However, the mathematical lower bound of ε is 0. In general, reservoirs with flatter side slopes have larger ε (Mitchell, 1962). Sugiyama et al. (1997) studied dozens of flood events in catchments of varying sizes and concluded that ε varies between 0.3 and 1 with an average of 0.6. Smaller ε corresponds to concave recession curves whereas ε larger than 1 corresponds to convex curves (Hammond and Han, 2006). Note that ε is dimensionless, and the dimension of parameter κ depends on ε and equals $[L]^{3-3\varepsilon}$ $[T]^{\varepsilon}$ where $[L]$ and $[T]$ are length and time dimensions, respectively.

Many previous works have similarly analyzed the physical interpretation of the exponent ε with a focus on the recession curves of nonlinear routing with no inflow (Botter et al., 2009; Boyd et al., 1979). With inflow, the effect of ε on the shape of the outflow hydrograph is more complex. If $\varepsilon = 1$, Eq. (2) becomes linear and, hence, Eq. (1) refers to linear reservoir routing. Most real-world hydrological systems, however, do not behave as linear storages (Dooge, 2005; Kim and Georgakakos, 2014). To address this limitation, many authors presented a variety of modeling approaches, such the cascading linear reservoirs (Chow et al., 1988; Nash, 1957), multilinear methods (Camacho and Lees, 1999; Perumal, 1992; Sahoo, 2013) and piecewise linear approximation of the nonlinear storage processes (Ostrowski, 2010). Basha (1995) offered an approximate solution via perturbation expansion around nominal ε. Glynn and Glynn (1996) presented a diffusion approximation for a network of nonlinear reservoirs with power-law release rules. To the best of the authors' knowledge, however, no exact general solutions have been reported to date for Eqs. (1) and (2) with $\varepsilon \neq 1$. A number of studies, including Hughes and Murrell (1986), Basha (1995), David (2009) and Del Giudice et al. (2014), suggested that no analytical solution exists for non-zero inflows unless ε equals 1/2 or 1. They presented several numerical solution methods and postulated that the accuracy of the solutions depends on the time interval used in the numerical integration. In this paper, we present an exact implicit solution for nonlinear routing of Eq. (1) with the general power-law storage function of Eq. (2) for constant inflow. The solution may be parametrized either by using statistical methods similarly to the Muskingum method (Linsley et al., 1949) or by using hydraulic properties of the channels similarly to the Muskingum-Cunge method (Chow et al., 1988). In this work, we expressed the power-law storage function parameters in terms of the hydraulic properties of the channels and the geometry of the storage structure. Because any real-world inflow hydrograph may be represented by a series of pulses of arbitrary widths, the exact solution is completely general. The proposed solution may therefore be used in a wide range of applications including modeling, design, forecasting and control of flow through single or cascades of reservoirs, and networks of channels. This paper is organized as follows. Section 2 presents the exact implicit solution of Eqs. (1) and (2). Section 3 presents the general expressions for the parameters of the power-law storage functions commonly encountered in reservoir and channel routing in the real world. Sections 4 and 5 present approximate explicit solutions and simple applications of the proposed solutions for different types of routing, respectively. Section 6 provides discussion. Section 7 presents the conclusions and future research recommendations.

2. Exact solution for nonlinear routing with power-law storage function

Using the chain rule, we may rewrite Eq. (1) as:

$$\frac{dQ}{dt} = \frac{I - Q}{dS/dQ} \tag{3}$$

If the storage function is of the power-law type of Eq. (2), there exist real-valued parameters a and b such that:

$$\frac{1}{dS/dQ} = aQ^b \tag{4}$$

where $a = 1/(\kappa\,\varepsilon)$ and $b = 1 - \varepsilon$. Combining Eqs. (3) and (4), we have the following nonhomogeneous nonlinear ordinary differential equation:

$$\frac{dQ}{dt} = aQ^b(I - Q) \tag{5}$$

where the parameter b is the dimensionless, and the parameter a has a dimension $[L]^{-3b}\ [T]^{b-1}$ where $[L]$ and $[T]$ are length and time dimensions, respectively.

Note that Eq. (5) is identical to the Horton-Izzard model (Dooge, 1973; Ponce, 2014) commonly used to model nonlinear overland flow. Moore and Bell (2001) described the application of Eq. (5) in operational flood forecasting in the United Kingdom and show the analogy between the nonlinear power-law storage function and the Horton-Izzard equation. They also postulated that such nonlinear storages commonly occur in many physical elements in the rainfall-runoff processes, and that it is reasonable to extend the nonlinear storage model to a wide range of "input-storage-output system" such as a soil column, aquifer storage or surface storage at catchment scale.

Various modeling efforts reported in the literature using the Horton-Izzard equation may be replicated with Eq. (5) following simple mathematical manipulations. For example, Moore and

Bell (2001) used an inverse definition of $Q = k\,S^m$ to describe specific discharge on a sloping plane following Dooge (1973) and Ponce et al. (1997). They also discussed how Horton introduced the "index of turbulence", $\frac{3\,(3-m)}{4}$ $\left(= \frac{3\,(2-3b)}{4(1-b)}\right)$, which ranges from 0 to 1, by combining the power-law storage function with the Manning's equation of sheet flow under the wide channel assumption. An index of turbulence of 0 results from $m = 3$ ($b = \frac{2}{3}$) and corresponds to laminar flow whereas an index of 1 results from $m = \frac{5}{3}$ ($b = \frac{2}{5}$) and indicates turbulent flow. The analytical solution for the Horton-Izzard model exists only for rational values of m and closed-form solutions existed only for specific values of m (Gill, 1977, 1976; Jolley and Wheater, 1997; Moore et al., 2005; Moore and Bell, 2002, 2001). For this reason, researchers and practitioners have frequently been forced to approximate m and optimize k. For instance, the Thames Catchment Model (Young, 1997) uses the analytical solution to the quadratic storage model ($\varepsilon = 1/2$). The PDM model (Young, 1997) uses an approximate recursive solution based on a piecewise linear difference equation to solve the cubic storage function ($\varepsilon = 2/3$). Meert et al. (2016) also used a piecewise linearization approach. The general solution removes such approximations and complications. The subsections below provide the exact solutions for Eq. (5) and, by extension, the Horton-Izzard nonlinear storage equation.

2.1. Outflow smaller than non-zero inflow

Introducing $q = Q/I$ and using separation of variables, we may rewrite Eq. (5) as follows for a sufficiently short time interval over which the inflow I may be assumed constant:

$$\frac{dq}{q^b(1-q)} = aI^b dt \qquad (6)$$

To integrate the left-hand side (LHS) of Eq. (6), we note that the denominator therein is the integrand of the incomplete beta function (IBF) (Dutka, 1981):

$$\beta_x(u,w) = \int_0^x \phi^{u-1}(1-\phi)^{w-1}\, d\phi, \qquad 0 \le x < 1 \tag{7}$$

where u and v are either positive real numbers or negative integers (Al-Sirehy and Fisher, 2013). Assigning $u = 1 - b$ and $w = 0$ in Eq. (7), substituting Q/I for q in the LHS of Eq. (6) and prescribing $Q(t_0) = Q_0$ as the initial condition (IC) of Eq. (5), we obtain the following exact implicit solution for Q:

$$\beta_{Q/I}(1-b,0) - \beta_{Q_0/I}(1-b,0) = aI^b(t-t_0), \qquad Q_0 < I \tag{8}$$

With $b = 1 - \varepsilon$, the above solution may be expressed in terms of the exponent ε in the storage-discharge relation. Note that the real-world domain of $\varepsilon > 0$ matches the mathematical domain of $b < 1$ as required by the IBF.

Eq. (8) may be used to obtain the outflow Q due to an arbitrary inflow hydrograph I discretized into a series of constant pulses I_{t_i}. Solving for Q in Eq. (8) amounts to nonlinear root finding for which one may use a combination of look-up tables for evaluation of the IBFs and iterative numerical algorithms (Al-Sirehy and Fisher, 2013). Once the calculation for a pulse of inflow is complete, one may continue to the next pulse, $I_{t_{i+1}}$, with Q_0 and t_0 in Eq. (8) reinitialized. Because $\beta_x(u,w)$ is real-valued for $0 < x < 1$ only, Eq. (8) is applicable only if $Q_0 < I_{t_i}$. If the outflow exceeds the constant inflow, it is necessary to use a second solution, which is described below.

2.2. Outflow larger than non-zero inflow

When the initial value of outflow, Q_0, is larger than the constant inflow I, a change of variable of $q^* = I/Q$ may be used to rewrite Eq. (5) in terms of q^* as follows:

$$\frac{dq^*}{{q^*}^{1-b}(1-q^*)} = aI^b dt \tag{9}$$

Assigning $u = b$ and $w = 0$ in Eq. (7), substituting I/Q for q^* in the LHS of Eq. (9), and prescribing $Q(t_0) = Q_0$ as the IC, one arrives at the following exact implicit solution for $Q > I$:

$$\beta_{I/Q}(b,0) - \beta_{I/Q_0}(b,0) = a\, I^b(t-t_0), \qquad Q > I \tag{10}$$

2.3. Zero inflow

When there is no inflow, i.e. $I = 0$, the analytic solutions above are no longer applicable. Instead, one may simplify Eq. (5) to:

$$\frac{dQ}{dt} = -aQ^{b+1} \tag{11}$$

Eq. (11) may be integrated via separation of variables to yield the following exact solution for Q which represents the recession curve for nonlinear reservoir with a general power-law storage function:

$$Q(t) = \left(\frac{1}{Q_0^b} + ab(t-t_0)\right)^{-\frac{1}{b}} \tag{12}$$

Once Q is determined, the associated storage may also be evaluated by integrating Eq. (4):

$$S(Q) = S_0 + \frac{Q^{1-b} - Q_0^{1-b}}{a(1-b)} \tag{13}$$

where S_0 denotes the initial storage. Eq. (13) is useful for checking for the full capacity condition when there exists an upper bound to the physical storage space.

2.4. Special case of integer b values

For integer values of the exponent *b*, simpler solutions exist via the extension of the conventional IBF (Özçağ et al., 2008):

$$\beta_x(\eta, 0) = -ln(1-x) - \sum_{i=1}^{n-1} \frac{x^i}{i} \tag{14}$$

$$\beta_x(-\eta, 0) = ln\frac{x}{1-x} - \sum_{i=1}^{n} \frac{x^{-i}}{i} \tag{15}$$

where $\eta = 1, 2, \cdots$. When b is an integer, Eqs. (14) and (15) may be used to replace the LHS of Eqs. (8) and (10). The right-hand side of Eqs. (14) and (15) are a generalization of the previously known analytical solutions of Moore and Bell (2002). A commonly encountered but particularly interesting case is when $b = -1$ as in reservoirs with linear storage-elevation relationships and a single orifice or submerged sluice gate outlet. Using Eq. (15), one may show that the nonlinear routing with power-law storage function has a compact explicit analytical solution expressed in terms of the Lambert W function, $W(\,)$ (Corless et al., 1996):

$$Q(t) = I\left(1 + W\left(\frac{(Q_0 - I)e^{\frac{Q_0 - a(t-t_0) - I}{I}}}{I}\right)\right) \tag{16}$$

Known also as the Lambert–Euler omega function (Pudasaini, 2011), the Lambert W function appears in the solution of many real-world problems (Corless et al., 1996; P. et al., 2000; Scott et al., 2006). It is worth noting that the Lambert W function has also been used in the similarity solution of the Richards equation, explicit expressions for Green-Ampt infiltration rate (Barry et al., 1993; Li et al., 2015; Parlange et al., 2002 to name a few), exact solutions for debris and avalanche flows (Pudasaini, 2011) and shallow flow in sloping unconfined aquifers (Barnes, 2018).

3. Storage function parameters

To use the above solution, it is necessary to specify the parameters a and b. Except when simple geometries are involved, the best approach in most practical applications is to calibrate them using observed inflow and outflow (see Wittenberg, 1994) . For those cases with known simple geometries or where calibration is not possible, theoretical expressions may be used. This section presents the theoretical parameters for widely used reservoir and channel routing applications.

3.1. For reservoir routing

The storage-elevation relationship is assumed to follow the power-law function below:

$$S = S_b + \sigma H^{\tau}, \qquad H \geq 0 \tag{17}$$

where S_b (m^3) denotes the reservoir volume below the outlet, H(m) denotes the elevation above the outlet, and σ and τ denote the power-law parameters approximating the volume of the reservoir above the outlet. In the following, S_b is assumed zero for the sake of simplicity. The width of the reservoir above the outlet structure, B (m), is also assumed to follow a power-law function:

$$B = \omega_0 H^{\omega_1}, \;\; \omega_0 > 0 \; and \;\; \omega_1 \geq 0 \tag{18}$$

The reservoir's cross-sectional area, A_y (m^2), may be obtained by integrating B over H:

$$A_y = \frac{\omega_0}{1+\omega_1} H^{1+\omega_1}, \qquad H \geq 0 \tag{19}$$

The storage-elevation relationship of Eq. (17) may now be written as:

$$S = A_y L_x = \frac{L_x \omega_0}{1+\omega_1} H^{1+\omega_1}, \qquad H \geq 0 \tag{20}$$

where L_x (m) denotes the longitudinal dimension of the reservoir. To describe the outflow as a function of flow depth, a power-law rating curve is used:

$$Q = r_0 H^{r_1}, \qquad H \geq 0 \tag{21}$$

If the reservoir has an overflow spillway, its outflow follows the weir equation (Chanson, 2004) with $r_0 = \frac{2}{3} C_d L_s \sqrt{2g}$ and $r_1 = 1.5$ where C_d denotes the coefficient of discharge, L_s(m) denotes the length of spillway perpendicular to direction of flow, and g denotes the gravitational acceleration (~ 9.81 m/s^2). If the reservoir has an orifice spillway, its outflow follows the orifice equation (Chanson, 2004) with $r_0 = C_d A_0 \sqrt{2g}$ and $r_1 = 0.5$ where A_0 (m^2) denotes the area of the orifice. Substituting Eq. (21) in Eq. (4), differentiating the LHS with respect to Q, and equating with the RHS, one has for the storage function parameters a and b:

$$a = \frac{r_1 r_0^{\frac{\omega_1+1}{r_1}}}{L_x \omega_0}, \text{ and } b = 1 - \frac{\omega_1+1}{r_1} \tag{22}$$

Notice that the combination of $\omega_1 = 0$ (i.e. linear storage-elevation relationship) and $r_1 = 0.5$ (e.g. orifices or submerged openings in sluice gates) results in $b = -1$ for which the nonlinear routing problem with power-law function admits the explicit solution of Eq. (16) in terms of the Lambert W function.

3.2. For channel routing

The Horton-Izzard equation has been widely used to model overland flows (Moore and Bell, 2001). If the simplifying assumption of level pool routing is justified (see, e.g., Fread and Hsu, 1993 for criteria), the power-law storage function may be derived for channel routing using the hydraulic properties of channels as described below. The flow resistance equation for wide channels combines the geometric properties of the channel cross section and flow properties (Menabde and Sivapalan, 2001; Yen, 2002):

$$v = c_0 y^{c_1} S_0^{c_2} \tag{23}$$

where v (m/s) denotes the mean velocity, y (m) denotes the depth, and S_0 (m/m) denotes the slope. In the above, c_0 , c_1, and c_2 are the flow resistance equation coefficients given by $c_0 = 1/n$, $c_1 = 2/3$, and $c_2 = 1/2$ for the Manning's equation, $c_0 = C$, $c_1 = 1/2$ and $c_2 = 1/2$ for the Chezy equation, and $c_0 = \sqrt{8g/f}$, $c_1 = 1/2$ and $c_2 = 1/2$ for the Darcy-Weisbach equation where n (s/ m$^{1/3}$), C (m$^{1/2}$/s) , and f (dimensionless) denote the respective roughness coefficient. The cross-sectional area of the channel, A (m^2), is approximated by a power-law function:

$$A = a_0 y^{a_1} \tag{24}$$

where a_0 and a_1 are the parameters of the power-law cross section. For example, for a rectangular channel, a_0 is the width of the channel and a_1 is unity. The discharge is given by the continuity equation:

$$Q = Av = a_0 c_0 y^{a_1 + c_1} S_0^{c_2} \tag{25}$$

Solving Eq. (25) for the depth y gives:

$$y = \left(\frac{Q}{a_0 c_0 S_0^{c_2}} \right)^{\frac{1}{a_1 + c_1}} \tag{26}$$

Assuming that the change in depth over the channel is not very large and the unsteadiness of flood wave has a wavelength larger than the channel length L (m), the storage, S (m^3), in the channel is given by (McCuen, 2004):

$$S = AL = a_0 L y^{a_1} \tag{27}$$

Substituting Eq. (26) in Eq. (27) and rearranging, one has for S:

$$S = Lc_0^{\frac{-a_1}{a_1+c_1}} a_0^{\frac{c_1}{a_1+c_1}} S_0^{\frac{-a_1 c_2}{a_1+c_1}} Q^{\frac{a_1}{a_1+c_1}} \tag{28}$$

Using Eq. (28), one may write the parameters a and b in Eq. (4) as:

$$a = \frac{a_1 + c_1}{a_1 L} c_0^{\frac{a_1}{a_1+c_1}} a_0^{\frac{-c_1}{a_1+c_1}} S_0^{\frac{a_1 c_2}{a_1+c_1}}, and\ b = \frac{c_1}{a_1 + c_1} \tag{29}$$

In the above development, the parameters a and b are determined by the flow resistance equation of choice. In practice, they may be prescribed empirically based on actual observations. For hillslope flow, there may not exist the necessary physiographic information to prescribe the parameters. In such cases, one may use the fractal relationships if self-similarity holds for the hillslope networks (Menabde and Sivapalan, 2001).

4. Approximate explicit solutions

The exact solution, Eq. (8), is in an implicit form. For practical applications, an explicit solution, which requires inversion of the IBF, is highly desirable. To the best of authors' knowledge, a compact explicit approximation does not exist for the inverse of the IBF. In this section, we offer symbolic approximations instead. The above inverse problem is equivalent to finding the function $Y = \Psi(X, b)$ such that:

$$\beta_Y(1 - b, 0) = X \tag{30}$$

The nonlinear routing problem is thus transformed into evaluating the Ψ function in the following expression:

$$\frac{Q(t)}{I} = \Psi\left(\beta_{Q_0/I}(1 - b, 0) + aI^b(t - t_0), b\right) \tag{31}$$

Below, we approximate $\Psi(\ )$ to solve nonlinear routing with power-law storage explicitly.

4.1. Compact expression for rising limb

To the best of our knowledge, approximations of the inverse of the IBF have not been reported in the literature. In this work, we use the following approximate inverse function developed via symbolic regression analysis. When the initial outflow is smaller than the inflow, i.e., $0 < X = \frac{Q(t)}{I} < 1$, we may approximate $\Psi_r(X,b)$ with:

$$\Psi_r(X,b) = \mathrm{erf}\left(\frac{1}{p_0 + p_1 X^{p_2}}\right), \qquad 0 < X = \frac{Q(t)}{I} < 1 \tag{32}$$

where erf( ) denotes the error function, and p_o, p_1, and p_2 denote the coefficients to be prescribed. For $-4 < b < 0.01$, Eq. (32) may be evaluated with a maximum error of 0.004 using the following symbolic solutions for p_0 to p_2:

$$\mathrm{p}_0 = 0.00330406\mathrm{b}^3 + 0.0385704\mathrm{b}^2 + 0.246985\mathrm{b} + 0.261149 \tag{33}$$

$$\begin{aligned} p_1 = {} & 0.00363074b^6 + 0.0494253b^5 + 0.270008b^4 \\ & +0.763024b^3 + 1.20429b^2 + 1.00517b + 1.29167 \end{aligned} \tag{34}$$

$$\begin{aligned} p_2 = {} & -0.00130776b^6 - 0.0185418b^5 - 0.107914b^4 \\ & -0.339224\,b^3 - 0.652824b^2 - 0.869868b - 0.9324260 \end{aligned} \tag{35}$$

For $0.01 < b < 0.7$, Eq. (32) has a maximum error of 0.007 when p_0 to p_2 are given by:

$$p_0 = 0.101487b^2 + 0.251458b + 0.264601 \tag{36}$$

$$p_1 = \exp(38.27b^4 - 35.5156b^3 + 14.4538b^2 - 0.665017b + 0.313546) \tag{37}$$

$$p_2 = -\exp(1.60103b^3 - 0.372287b^2 + 1.15131b - 0.0738377) \tag{38}$$

Because the level pool assumption puts the peak outflow on the inflow hydrograph, Eq. (32) may be used to approximate the peak outflow due to a constant inflow I_d (m^3/s), with duration t_d (s). For example, if the reservoir is initially empty, the peak outflow of Q_p(m^3/s) satisfies:

$$\frac{Q_p}{I_d} = \mathrm{erf}\left(\frac{1}{p_0 + p_1\left(aI_d{}^b t_d\right)^{p_2}}\right) \tag{39}$$

The peak storage S_p (m^3) may be approximated using Eq. (13) as:

$$S_p = S_0 + \frac{\left(\mathrm{erf}\left(\frac{1}{p_0 + p_1\left(aI_d{}^b t_d\right)^{p_2}}\right) I_d\right)^{1-b} - Q_0^{1-b}}{a(1-b)} \tag{40}$$

4.2. Series expansions for rising and falling limbs

Following Dominici (2005), an approximate expression for the inverse of the IBF may be obtained by a series expansion in the neighborhood of valid X_0. This approach utilizes the nested derivative operator defined as:

$$\mathfrak{D}^z[f](x) = \frac{d}{dx}\left[f(x) \times \mathfrak{D}^{z-1}[f](x)\right] \tag{41}$$

with $\mathfrak{D}^0[f](x) = 1$. Accordingly, the inverse function values for the rising and falling portions of the solution, $\Psi_\mathrm{r}(\,)$ and $\Psi_\mathrm{f}(\,)$, respectively, are given by:

$$\Psi_r(X, b) = X_0 + f_\mathrm{r}(X_0) \sum_{z \geq 1} \mathfrak{D}^{z-1}[f_\mathrm{r}](X_0) \frac{\left(X - \beta_{X_0}(1-b, 0)\right)^z}{z!},$$
$$f_\mathrm{r}(X_0) = (1 - X_0) X_0{}^b \tag{42}$$

$$\Psi_f(X, b) = X_0 + f_p(X_0) \sum_{z \geq 1} \mathfrak{D}^{z-1}\left[f_p\right](X_0) \frac{\left(X - \beta_{X_0}(b, 0)\right)^z}{z!},$$
$$f_p(X_0) = (1 - X_0) X_0{}^{1-b} \tag{43}$$

Care should be taken in choosing X_0 to ensure f_r and f_p have non-zero real values at that point. A faster but less accurate method is to choose a fixed X_0 throughout the entire simulation. A generally more accurate approach is to update X_0 at each time step with the latest known value from the previous time step. Another important factor in applying Eqs. (42) and (43) is the number of terms summed in the partial series. **Fig.** 1 shows the difference between the exact and approximated values of the inverse of the IBF for $\Psi_r(X,b)$ with $X_0 = 0.75$. The figure indicates that even a small number of terms in the series sum yields accurate results if the time increments are chosen for X to remain relatively close to X_0.

5. Applications

This section presents four simple applications of the above solutions to different types of routing problems. The first and second show the ability of the proposed solution in simulating laboratory-observed flows in reservoir and channel, respectively. The third uses the proposed solution for real-world river flood routing and compares with the observed flow and the S-V solution. The last application uses the approximate explicit solution for detention pond design.

5.1. Reservoir routing with orifice spillway

The laboratory data from Kilduff (2002) are used to validate the proposed solution. In this application, a constant inflow of 12.3 mL/s is applied to a cylindrical reservoir with a base area of 71 cm^2. The inflow is kept constant for a duration of 300 seconds and then shut off completely. The water surface elevation is observed above a 0.4 cm orifice with $H = \frac{Q^2}{19.131}$ where H denotes the elevation above the outlet in cm and Q denotes the discharge in cm^3/s. Using Eqs. (21) and (22), one has $a = 0.13473\ (cm^3 s^{-2})$ and $b = -1$. Solving Eq. (8) for H with a time step of 5 seconds, we have the adjusted coefficient of determination $\bar{R}^2$ of 0.993 with the observed water surface elevation (see **Fig.** 2). In the figure, there exists an outlying observed water level. Given that this case study is a simple laboratory experiment with well-known behavior, the outlier is likely to be an observational error. Since $b = -1$, Eq. (16) is applicable in this example and the routed hydrograph can be obtained implicitly in terms of the Lambert W function as $Q(t) = 12.3(W(-0.36788e^{-0.01095t}) + 1)$ for $t < 300$. After the inflow is shut off, Eq. (12) gives $Q(t) = 52.54739 - 0.13473t$ for $300 \leq t < 390$. Note that in this application the explicit analytical solution of Eq. (16) results in peak water level of 74.86 cm which is very close to the observed value of 75.03 cm. For comparison, the compact approximate solution of Eq. (32) yields a peak water level of 76.32 cm.

5.2. Level pool channel routing with significant floodplain storage

De Martino et al. (2012) assessed the assumption of level pool routing in an experimental channel. They confirmed via extensive experimental investigations that the level pool assumption may be reliably applied for floodplain storage and concluded that vegetation and channel bottom irregularities are larger sources of uncertainties in flood modeling than the level pool assumption. They also deduce that simple storage-based methods such as the ones presented in this paper are preferred for preliminary sizing of floodplain storages in flat areas. In the following, we validate the proposed solutions using the data from the out-of-bank portion of one of their experiments where the power-low equations hold true. In this test, the flow is out of bank during the period of 52 to 350 seconds. With the floodplain storage area of $A = 29.12\ m^2$, the storage-elevation relationship is linear with $S = 29.12\ H$. The outlet is a sluice gate with a 0.05 m opening. Using Eqs. (18) through (22), one arrives at $a = 6.98 \times 10^{-5}\ (m^3 s^{-2})$ and $b = -1$. Based on these values, the explicit solution of Eq. (16) is used with a time step of 10 seconds to predict the observed flows with $\bar{R}^2 = 0.951$ as shown in **Fig.** 3. Note that, from 52 to 212 seconds, the inflow is effectively constant for which the average value is 0.066 m^3/s. Given the initial outflow of 0.035 m^3/s, the Lambert W function-based explicit solution of Eq. (16) is able to predict the peak observed outflow of 0.043 m^3/s with only one calculation step.

5.3. Channel routing

In this example, a flash flooding event in a natural waterway was chosen from Akbari and Barati (2012). The channel has width of 10 m, slope of 0.0012, length of 25 km, and Manning's roughness of 0.035 s/ $m^{1/3}$. For this event, the observed inflow and outflow hydrographs are available as well as the S-V solution which is used here for additional comparison. **Fig.** 4 shows that the proposed solution with calibrated parameters of $a = 4.25 \times 10^{-4}$ $(m^{-0.5982}s^{-0.8006})$ and $b = 0.1994$, and a time step of 1 min is able to simulate the observed flows extremely closely ($\bar{R}^2 = 0.997$). Overall, the nonlinear storage routing compares well with the S-V solution. Not surprisingly, however, the shape of the hydrograph and the peak flow are less accurate than the S-V solution due to the level pool assumption which forces the peak outflow on the inflow hydrograph.

5.4. Detention pond design

In this application, the approximate explicit solution of Eq. (39) is used to design a detention pond. The pond has a 10 m-by-5 m rectangular base. It is desired to size an orifice outlet to reduce peak outflow for a 0.25 m^3/s inflow. The approximate solution of Eq. (39) may be used to estimate the reduction in peak outflow. The peak storage curves (see **Fig.** 5) obtained from Eq. (40) may be used to verify that the maximum available physical storage is not exceeded. Alternatively, given the dimensions of the pond and the orifice outlet, one may approximate the combined effect of changes in the magnitude and duration of inflow on the peak outflow. **Fig.** 6 shows the results with a 0.5 m-diameter outflow orifice.

6. Discussion

The main purpose of this study is to provide new analytical solutions for level pool routing with general power-law storage-discharge relationship, and to advance the theory of nonlinear hydrologic routing. A number of examples are presented to demonstrate the utility of the analytical solutions in a wide range of practical applications. If accuracy is of primary concern, the analytical solutions of Eqs. (8), (10), and (16) should be favored over numerical solutions. The choice of the routing method, however, depends on many other factors such as the validity of the underlying assumptions, nonlinearity of flow, availability of both real-time and historical data, parsimony desired, ease of implementation, and computational requirements and resources available. The relative importance of these factors is very often application-specific and hence the choice of the solution approach may vary significantly. Below we elaborate on the assumptions and limitations for the proposed solutions and offer computational considerations for implementation to aid such decision making. For comparisons among different numerical flood routing methods, the reader is referred to Strelkoff (1980), Ponce et al. (1997) and Ponce (2014).

Power-law storage function is a fundamental assumption for the presented solutions. As described in Section 3, these parameters represent the geometry and hydraulics in the storage-discharge relationship. In applying the solutions presented in this work, it is important that the power-law definitions are consistent with the formulations in Section 3 as alternative formulations are also possible. Note also that the solution presented is limited to the elevations above spillway, i.e., the surcharge storage (Viessman and Lewis, 2008). Power-law storage function is generally not consistent with multiple types of outlet structures but may still provide acceptable approximation.

If the power-law storage-discharge relationship is not sufficiently well modeled by a single set of coefficients, it may be necessary to employ multiple sets of the parameter estimates for local approximation. Such approaches are routinely practiced in operational river routing in the form of layered coefficient routing (Fread, 1985; NWS, 2021b). As such, the power-law assumption is not as large a limiting factor as it may first appear. As is often the case in practice, one may improve the accuracy by calibrating the two coefficients, or adjusting the a priori estimates obtained from the geometric and hydraulic considerations, based on observed hydrographs when and where available. It is also noted here that the IBF solution offers a potentially significant advantage in gradient-based parameter optimization over other numerical routing techniques because the derivatives can be evaluated very accurately.

The proposed solutions assume a level pool reservoir. It is widely accepted that level pool routing is more appropriate for smaller reservoirs with rounder shape where backwater effects are not significant (Chow et al., 1988; Ionescu and Nistoran, 2019). Level pool routing is also widely used for channel routing for which a reach is subdivided into a series of level pools with prescribed storage-discharge relationships (USACE, 2021). The degree of attenuation in the routed flood wave may vary depending on the number of sub-reaches chosen, which is often treated as a calibration parameter (Bonner, 1990; USACE, 1994). Level pool routing, and hence the proposed solutions, are not recommended for streams with gradients less than ~ 0.0004 to.0006, reaches with time-varying boundary conditions such as tides or rapidly rising flood hydrographs (Bonner, 1990; USACE, 1994).

The assumption of constant inflow is of little practical significance because the observed and simulated inflow hydrographs are already discretized according to the sampling interval of the instrument and the time step of the simulation, respectively. If the hydrograph is over-sampled such that the discharge varies very little over a short time period, one may coarsen the discretization to reduce the number of IBF evaluations. In such a case, the level of discretization should be chosen such that the sampling frequency captures the variations and peakedness in the inflow hydrograph.

The analytical solution requires evaluation of the IBF. If the IBF is not available as a built-in or intrinsic function in the user's computing environment, one may use external mathematical libraries (see for example http://www.meta-numerics.net/ and https://www.boost.org/). The main computing requirement for the analytical solution comes from solving for Q in the implicit expressions of Eqs. (8) and (10). The above nonlinear root finding problem may be solved using a number of readily available techniques (Faires and Burden, 2012). A potential difficulty in the above solution is slow convergence near the poles of the IBF but may be avoided by using derivative-free techniques. For example, with the bisection method (Faires and Burden, 2012), a conservative estimate for the number of iterations required to determine Q is $\log_2\left(\frac{|I-Q_0|}{TOL}\right)+1$ where TOL is the desired tolerance (Faires and Burden, 2012). Though there may exist more efficient methods, the bisection method is very attractive for the IBF, a strictly monotonically increasing function, owing to its simplicity and the availability of the a priori estimate for convergence.

Because the proposed solution is analytical, one does not have to be concerned about numerical errors or diffusion, and may hence expect to obtain extremely accurate solutions. To illustrate, below we offer a comparison of the proposed solution with a number of numerical integration schemes for an inflow hydrograph shown as a series of pulses in Fig 7. The example hydrograph is based on Fenton (2010) in which a small reservoir with square base of 100 m by

100 m and a weir outlet with a width of 4 m is subjected to an inflow hydrograph of the following general form:

$$I(t) = I_0 + (I_p - I_0)\left(\frac{t}{T_p}\, e^{\left(1-\frac{t}{T_p}\right)}\right)^5 \tag{44}$$

where I_0 is the initial inflow of 1 m^3/s, I_p is the peak inflow of 20 m^3/s, and T_p is the time to peak of 30 min. It follows from Section 3.1 that a is 0.000554 m^{3}s^{-2} and b is 0.31927. The above hydrograph is resampled at an interval of 300 s to emulate a discrete observed hydrograph in the real world. An accurate Method of Lines numerical solution with high-resolution adaptive mesh (Hamdi et al., 2007; Wolfram, 2021) is used to obtain the reference 'true' outflow hydrograph (see Fig 7). We then used the different solution methods shown in Table 1 to route the inflow hydrograph at time steps of 10, 30 and 60 s. The small time steps were chosen to ensure that the variations in the inflow hydrograph are captured for all solution techniques considered.

Fig. 7 shows the results for the analytical solution with $\Delta t = 60$ s vs. the reference truth. As expected, they are indistinguishably close. Table 1 shows the maximum errors in percent in the proposed and numerical solutions for the duration of the hydrograph. Because all three time steps are smaller than the sampling interval of the inflow hydrograph (i.e., 300 s), the analytical solution results are effectively the same for all time steps. The maximum errors in the numerical solutions, on the other hand, show significant sensitivity to the time step and vary significantly among themselves. It is seen that the higher-order solutions tend to be more accurate among the numerical solutions, and that the proposed solution is far more accurate than any of the numerical solutions even at the smallest time step of 10 s.

Time Step	$\Delta t = 10$ s	$\Delta t = 30$ s	$\Delta t = 60$ s
Incomplete Beta Function (Proposed Solution)	-0.000076%	-0.000076%	-0.000076%

Euler (Order=1)	-3.159%	-8.931%	-16.43%
Midpoint (Order=2)	-0.00469%	-0.04219%	-0.1687%
Runge-Kutta (Order=2)	-1.589%	-4.497%	-8.277%
Runge-Kutta (Order=3)	-0.5298%	-1.503%	-2.788%
Runge-Kutta (Order=4)	0.1123%	0.9001%	3.05%

Table 1- Maximum error of routing solution for the test inflow shown in Fig 7.

7. Conclusions and future research recommendations

An exact implicit solution for nonlinear reservoir routing with a general power-law storage function is presented. Expressed in terms of the incomplete beta function (IBF), the solution is valid for inflow hydrographs that may be represented by a series of pulses of arbitrary widths. The solution thus extends the existing analytical solutions reported in the literature which are valid only for specific exponents in the power-law storage function. For reservoirs with linear storage-elevation relationship and a single orifice or submerged sluice gate outlet, an explicit compact solution expressed in terms of the Lambert-W function is presented. To facilitate the application of the new solution to reservoir and channel routing, the two power-law storage function parameters are expressed in terms of the geometry of the reservoir, rating curve, and flow resistance. The exact solution applies only for constant inflow and is in an implicit form for the general case. For practical applications, several highly-accurate, approximate explicit solutions are also presented. To demonstrate the accuracy and utility of the new solutions, four simple applications are presented for reservoir routing, channel routing, and detention pond design. Being exact, the new solution is not subject to numerical errors or instabilities. It is therefore particularly useful in nonlinear routing applications when accuracy is of particular importance. The solution may also be useful in network or system optimization as well as design analysis that requires derivatives.

8. Funding

This work was supported by the National Science Foundation under Grant CyberSEES-1442735; and by the National Oceanic and Atmospheric Administration's Joint Technology Transfer Initiative Program under Grant NA17OAR4590184. These supports are gratefully acknowledged.

9. References

Al-Sirehy, F., Fisher, B., 2013. EVALUATION OF THE BETA FUNCTION. Int. J. Apllied Math. 26. https://doi.org/10.12732/ijam.v26i1.6

Ayalew, T.B., Krajewski, W.F., Mantilla, R., Small, S.J., 2014. Exploring the effects of hillslope-channel link dynamics and excess rainfall properties on the scaling structure of peak-discharge. Adv. Water Resour. 64, 9–20.

Barnes, R.J., 2018. Shallow Unconfined Flow on a Sloping Base Redux. Groundwater 56, 610–617. https://doi.org/10.1111/gwat.12607

Barry, D.A., Parlange, J.-Y., Sander, G.C., Sivaplan, M., 1993. A class of exact solutions for Richards' equation. J. Hydrol. 142, 29–46. https://doi.org/10.1016/0022-1694(93)90003-R

Basha, H.A., 2000. Simple Nonlinear Rainfall-Runoff Model. J. Hydrol. Eng. 5, 25–32. https://doi.org/10.1061/(ASCE)1084-0699(2000)5:1(25)

Basha, H.A., 1995. Routing Equations for Detention Reservoirs. J. Hydraul. Eng. 121, 885–888. https://doi.org/10.1061/(asce)0733-9429(1995)121:12(885)

Basha, H.A., 1994. Nonlinear Reservoir Routing: Particular Analytical Solution. J. Hydraul. Eng. 120, 624–632. https://doi.org/10.1061/(asce)0733-9429(1994)120:5(624)

Bentura, P.L.F., Michel, C., 1997. Flood routing in a wide channel with a quadratic lag-and-route method. Hydrol. Sci. J. 42, 169–189. https://doi.org/10.1080/02626669709492018

Bonner, V.R., 1990. River Routing with HEC-1 and HEC-2. HYDROLOGIC ENGINEERING CENTER DAVIS CA.

Botter, G., Porporato, A., Rodriguez-Iturbe, I., Rinaldo, A., 2009. Nonlinear storage-discharge relations and catchment streamflow regimes. Water Resour. Res. 45. https://doi.org/10.1029/2008WR007658

Boyd, M.J., Pilgrim, D.H., Cordery, I., 1979. A storage routing model based on catchment geomorphology. J. Hydrol. 42, 209–230.

Camacho, L.A., Lees, M.J., 1999. Multilinear discrete lag-cascade model for channel routing. J. Hydrol. 226, 30–47.

Carter, R.W., Godfrey, R.G., 1960. Storage and Flood Routing: Manual of Hydrology: Part 3, Flood-flow Techniques. US Department of the Interior, Geological Survey.

Chanson, H., 2004. Hydraulics of open channel flow. Elsevier.

Chi, C.C., George, C., Ricardo, M., 2015. Implementation of a Hydraulic Routing Model for Dendritic Networks with Offline Coupling to a Distributed Hydrological Model. J. Hydrol. Eng. 20, 4015023. https://doi.org/10.1061/(ASCE)HE.1943-5584.0001152

Chow, V. Te, Maidment, D.R., Mays, L.W., 1988. Applied Hydrology. McGraw-Hill.

Corless, R.M., Gonnet, G.H., Hare, D.E.G., Jeffrey, D.J., Knuth, D.E., 1996. On the LambertW function. Adv. Comput. Math. 5, 329–359. https://doi.org/10.1007/BF02124750

Cunge, J.A., 1969. On the subject of a flood propagation computation method (Musklngum method). J. Hydraul. Res. 7, 205–230.

David, G.S., 2009. Generalized Numerical Solution for Detention Basin Design. J. Irrig. Drain. Eng. 135, 487–492. https://doi.org/10.1061/(ASCE)IR.1943-4774.0000010

De Martino, G., De Paola, F., Fontana, N., Marini, G., Ranucci, A., 2012. Experimental assessment of level pool routing in preliminary design of floodplain storage. Sci. Total Environ. 416, 142–147. https://doi.org/10.1016/j.scitotenv.2011.11.032

Del Giudice, G., Gargano, R., Rasulo, G., Siciliano, D., 2014. Preliminary Estimate of Detention Basin Efficiency at Watershed Scale. Water Resour. Manag. 28, 897–913. https://doi.org/10.1007/s11269-014-0518-1

Dominici, D., 2005. Nested Derivatives: A simple method for computing series expansions of inverse functions. arXiv:math/0501052.

Dooge, J., 1973. Linear theory of hydrologic systems. Agricultural Research Service, US Department of Agriculture.

Dooge, J.C.I., 2005. Bringing it all together. Hydrol. Earth Syst. Sci. 9, 3–14. https://doi.org/10.5194/hess-9-3-2005

Dutka, J., 1981. The incomplete Beta function—a historical profile. Arch. Hist. Exact Sci. 11–29.

Faires, J.D., Burden, R.L., 2012. Numerical Methods, 4th. Cengage Learning.

Fenton, J., 2010. Computational hydraulics. Dispon. en la siguiente Dir. http//luk. Staff. ugm. ac. id/hidkom/pdf/Computat ional-Hydraulics. pdf.

Fread, D.L., 1985. Channel routing. Hydrol. Forecast. by MG Anderson TP Burt.

Fread, D.L., Hsu, K.S., 1993. Applicability of Two Simplified Flood Routing Methods: Level-Pool and Muskingum-Cunge, in: Hydraulic Engineering. ASCE, pp. 1564–1568.

Fread, D.L., McMahon, G.F., Lewis, J., 1978. Limitations of Level-Pool Routing in Reservoirs. ASCE, pp. 227–238.

Gill, M.A., 1977. Algebraic solution of the Horton-Izzard turbulent overland flow model of the rising hydrograph. Hydrol. Res. 8, 249–256.

Gill, M.A., 1976. Exact solution of gradually varied flow. J. Hydraul. Div. 102, 1353–1364.

Glynn, J.E., Glynn, P.W., 1996. A diffusion approximation for a network of reservoirs with power law release rule. Stoch. Hydrol. Hydraul. 10, 17–37.

Goodell, C.R., Wahlin, B., 2009. Dynamic and level pool reservoir drawdown: A practical comparison for dam breach modeling. pp. 6843–6850.

Goodrich, R.D., 1931. Rapid calculation of reservoir discharge. Civ. Eng 1, 417–418.

Gupta, V.K., 2004. Emergence of statistical scaling in floods on channel networks from complex runoff dynamics. Chaos, Solitons & Fractals 19, 357–365.

Gupta, V.K., Waymire, E.C., 1998. SOME MATHEMATICAL ASPECTS OF RAINFALL, LANDFORMS, AND FLOODS. pp. 129–171. https://doi.org/10.1142/9789812839725_0005

Hamdi, S., Schiesser, W.E., Griffiths, G.W., 2007. Method of lines. Scholarpedia 2, 2859.

Hammond, M., Han, D., 2006. Recession curve estimation for storm event separations. J. Hydrol. 330, 573–585.

Hughes, D.A., Murrell, H.C., 1986. Non-linear runoff routing—a comparison of solution methods. J. Hydrol. 85, 339–347.

Ionescu, C.S., Nistoran, D.E.G., 2019. Influence of reservoir shape upon the choice of Hydraulic vs. Hydrologic reservoir routing method, in: E3S Web of Conferences. EDP Sciences, p. 7001.

Jolley, T.J., Wheater, H.S., 1997. The introduction of runoff routing into large-scale hydrological models. Hydrol. Process. 11, 1917–1926. https://doi.org/10.1002/(SICI)1099-1085(199712)11:15<1917::AID-HYP539>3.0.CO;2-W

Kilduff, J., 2002. Demonstrating Reservoir Routing in the Classroom: Physical and Mathematical Modeling. p. 1.

Kim, D.H., Georgakakos, A.P., 2014. Hydrologic routing using nonlinear cascaded reservoirs. Water Resour. Res. 50, 7000–7019.

Li, J., Wang, Z., Liu, C., 2015. A combined rainfall infiltration model based on Green–Ampt and SCS-curve number. Hydrol. Process. 29, 2628–2634. https://doi.org/10.1002/hyp.10379

Linsley, R.K., Kohler, M.A., Paulhus, J.L.H., 1949. Applied hydrology, 1st ed. ed. New Delhi : Tata McGraw-Hill.

Mandapaka Venkata, P., 2009. Role of rainfall variability in the statistical structure of peak flows. Theses Diss. https://doi.org/10.17077/etd.w2kxr15l

Mantilla, R., Gupta, V.K., 2005. A GIS numerical framework to study the process basis of scaling statistics in river networks. IEEE Geosci. Remote Sens. Lett. 2, 404–408. https://doi.org/10.1109/LGRS.2005.853571

Mantilla, R., Gupta, V.K., Mesa, O.J., 2006. Role of coupled flow dynamics and real network structures on Hortonian scaling of peak flows. J. Hydrol. 322, 155–167.

Mazzoleni, M., Noh, S.J., Lee, H., Liu, Y., Seo, D.J., Amaranto, A., Alfonso, L., Solomatine, D.P., 2018. Real-time assimilation of streamflow observations into a hydrological routing model: effects of model structures and updating methods. Hydrol. Sci. J. 63, 386–407. https://doi.org/10.1080/02626667.2018.1430898

McCarthy, G.T., 1938. The unit hydrograph and flood routing, in: Conference of the North Atlantic Division of US Corporations of Engineers.

McCuen, R.H., 2004. Hydrologic Analysis and Design. J. Am. Water Resour. Assoc. 40, 838.

Meert, P., Willems, P., Nossent, J., Vanderkimpen, P., Pereira, F., Verwaest, T., Mostaert, F.,

2016. Development of conceptual models for an integrated catchment management: subreport 3. Construction and calibration of conceptual river models. WL Rapp.

Menabde, M., Sivapalan, M., 2001. Linking space–time variability of river runoff and rainfall fields: a dynamic approach. Adv. Water Resour. 24, 1001–1014.

Mitchell, W.D., 1962. Effect of reservoir storage on peak flow. USGPO,.

Moore, R.J., Bell, V.A., 2002. Incorporation of groundwater losses and well level data in rainfall-runoff models illustrated using the PDM.

Moore, R.J., Bell, V.A., 2001. Comparison of rainfall-runoff models for flood forecasting. Part 1: Literature review of models.

Moore, R.J., Bell, V.A., Jones, D.A., 2005. Forecasting for flood warning. Comptes Rendus Geosci. 337, 203–217.

Nash, J.E., 1957. The form of the instantaneous unit hydrograph. Int. Assoc. Sci. Hydrol. Publ 3, 114–121.

Noh, S., Seo, D.-J., RafieeiNasab, A., McCreight, J., Gochis, D., Cosgrove, B., Vukicevic, T., 2018. Assimilation of Real-Time Streamflow Observations for the National Water Model Using Ensemble Kalman Filter.

Nourani, V., Singh, V.P., Delafrouz, H., 2009. Three geomorphological rainfall–runoff models based on the linear reservoir concept. Catena 76, 206–214.

NWS, 2021a. Office of Water Prediction [WWW Document]. NOAA/NWS/Office Water Predict. URL https://water.noaa.gov/about/nwm (accessed 1.28.21).

NWS, 2021b. OHD/HL - The National Weather Service River Forecast System User Manuals and On-line Doc [WWW Document]. NOAA/NWS/Office Water Predict. URL https://www.weather.gov/owp/oh_hrl_general_indexdoc (accessed 1.30.21).

Orlandini, S., Rosso, R., 1998. Parameterization of stream channel geometry in the distributed modeling of catchment dynamics. Water Resour. Res. 34, 1971–1985. https://doi.org/10.1029/98WR00257

Ostrowski, M., 2010. A generic Mathamatical Formulation of A piecewise Linear Approximation of Nonlinear Hydrological Storage Processes. preparation.

Özçağ, E., Ege, İ., Gürçay, H., 2008. An extension of the incomplete beta function for negative integers. J. Math. Anal. Appl. 338, 984–992. https://doi.org/10.1016/j.jmaa.2007.05.075

P., F.D., Keith, W., Ceri, D.L., J.S., C.A., Massimo, P., 2000. Quantitative General Theory for Periodic Breathing in Chronic Heart Failure and its Clinical Implications. Circulation 102, 2214–2221. https://doi.org/10.1161/01.CIR.102.18.2214

Parlange, J.-Y., Barry, D.A., Haverkamp, R., 2002. Explicit infiltration equations and the Lambert W-function. Adv. Water Resour. 25, 1119–1124. https://doi.org/10.1016/S0309-1708(02)00051-9

Perumal, M., 1992. Multilinear Muskingum flood routing method. J. Hydrol. 133, 259–272.

Ponce, V.M., 2014. Engineering hydrology: Principles and practices.

Ponce, V.M., Cordero-Brana, O.I., Hasenin, S.Y., 1997. Generalized conceptual modeling of dimensionless overland flow hydrographs. J. Hydrol. 200, 222–227.

Pudasaini, S.P., 2011. Some exact solutions for debris and avalanche flows. Phys. Fluids 23, 43301. https://doi.org/10.1063/1.3570532

Reggiani, P., Sivapalan, M., Hassanizadeh, S.M., Gray, W.G., 2001. Coupled equations for mass and momentum balance in a stream network: theoretical derivation and computational experiments. Proc. R. Soc. London. Ser. A Math. Phys. Eng. Sci. 457, 157–189.

Sahoo, B., 2013. Field application of the multilinear Muskingum discharge routing method.

Water Resour. Manag. 27, 1193–1205.

Scott, T.C., Mann, R., Martinez II, R.E., 2006. General relativity and quantum mechanics: towards a generalization of the Lambert W function A Generalization of the Lambert W Function. Appl. Algebr. Eng. Commun. Comput. 17, 41–47. https://doi.org/10.1007/s00200-006-0196-1

Small, S.J., Jay, L.O., Mantilla, R., Curtu, R., Cunha, L.K., Fonley, M., Krajewski, W.F., 2013. An asynchronous solver for systems of ODEs linked by a directed tree structure. Adv. Water Resour. 53, 23–32.

Sugiyama, H., Kadoya, M., Nagai, A., Lansey, K., 1997. Evaluation of the storage function model parameter characteristics. J. Hydrol. 191, 332–348.

Szymkiewicz, R., 2010. Numerical modeling in open channel hydraulics. Springer Science & Business Media.

Tallaksen, L.M., 1995. A review of baseflow recession analysis. J. Hydrol. 165, 349–370.

Todini, E., Ciarapica, L., 2001. The TOPKAPI model. Math. Model. large watershed Hydrol. 471–506.

USACE, 2021. Modified Puls Model [WWW Document]. HEC-HMS Tech. Ref. Man. URL https://www.hec.usace.army.mil/confluence/hmsdocs/hmstrm/channel-flow/modified-puls-model (accessed 1.30.21).

USACE, 1994. Flood Runoff Analysis. Em 1110-2-1417 214.

Viessman, W., Lewis, G.L., 2008. Introduction to Hydrology. PHI Learning Private.

Wittenberg, H., 1994. Nonlinear analysis of flow recession curves. J. Hydrol. 158, 405–406.

Wolfram, 2021. The Numerical Method of Lines—Wolfram Language Documentation [WWW Document]. URL https://reference.wolfram.com/language/tutorial/NDSolveMethodOfLines.html (accessed 1.30.21).

Yen, B.C., 2002. Open Channel Flow Resistance. J. Hydraul. Eng. 128, 20–39. https://doi.org/10.1061/(asce)0733-9429(2002)128:1(20)

Young, A.R., 1997. BENCH MARKING RAINFALL RUNOFF MODELS WITHIN THE ANGLIAN REGION FINAL REPORT. Wallingford.

Yu, G., Lim, S.-Y., 2003. Modified Manning formula for flow in alluvial channels with sand-beds. J. Hydraul. Res. 41, 597–608. https://doi.org/10.1080/00221680309506892

List of Figure Captions

Fig.1. An example of approximation error for various number of terms of Eq. (42) for X 0 =0.75 and b=-0.67.

Fig.2. Calculated and observed water levels of Example 1.

Fig.3. Comparison of calculated outflows with observed values of Example 2.

Fig.4. Comparison of the proposed solution vs. S-V solution for Example 3.

Fig.5. Peak storage as a function of inflow duration and orifice diameter.

Fig.6. Peak flow as a function of inflow duration and inflow magnitude.

Fig.7. An example inflow function was produced by resampling Eq. (44) to emulate a discrete observed hydrograph in the real world. The results from the proposed analytical solution applied at Δt=60 s intervals can closely simulate the accurate benchmark solution.

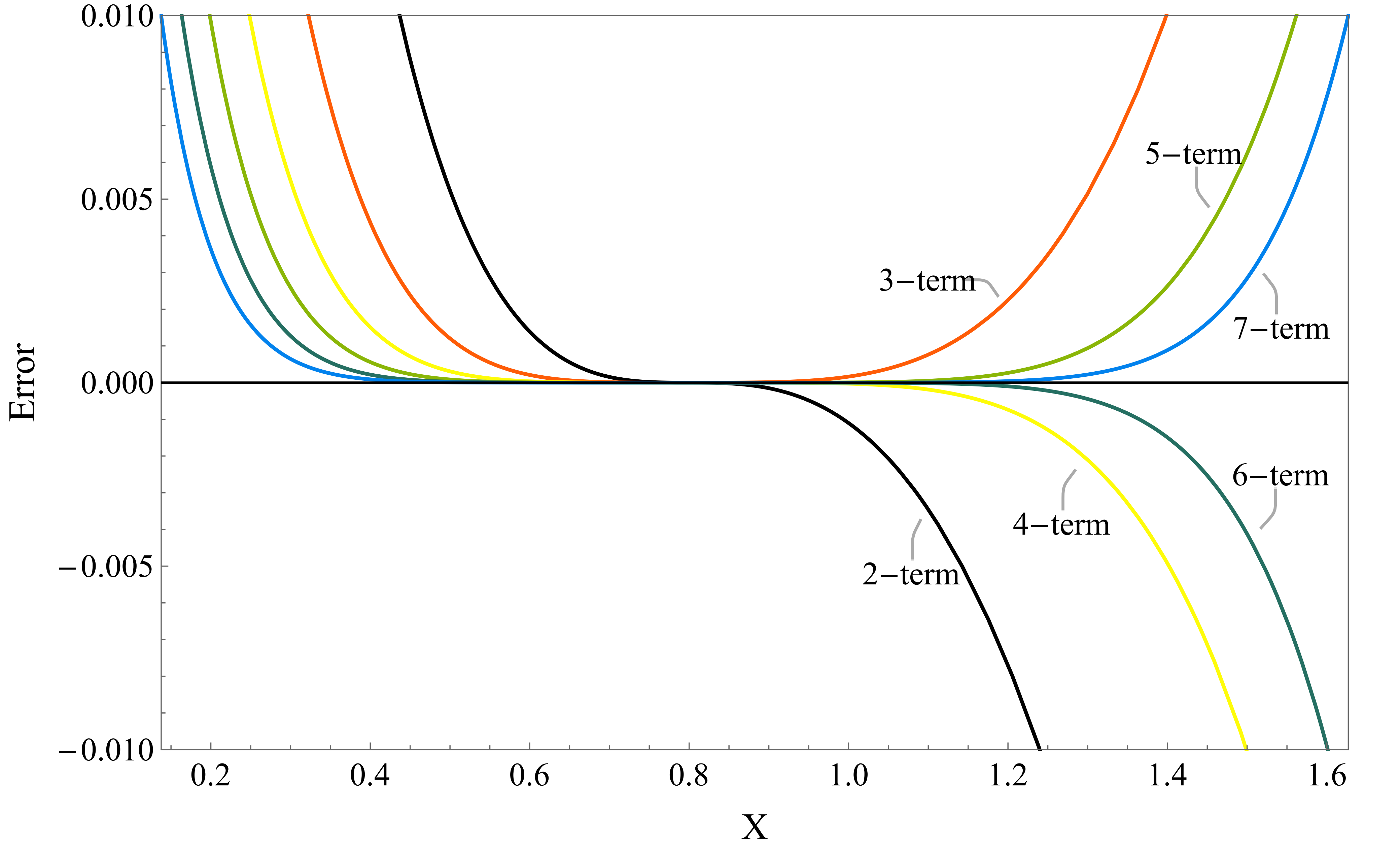

0.010
0.005
0.000
−0.005
−0.010
Error
0.2
0.4
0.6
0.8
1.0
1.2
1.4
1.6
X
2−term
3−term
4−term
5−term
6−term
7−term

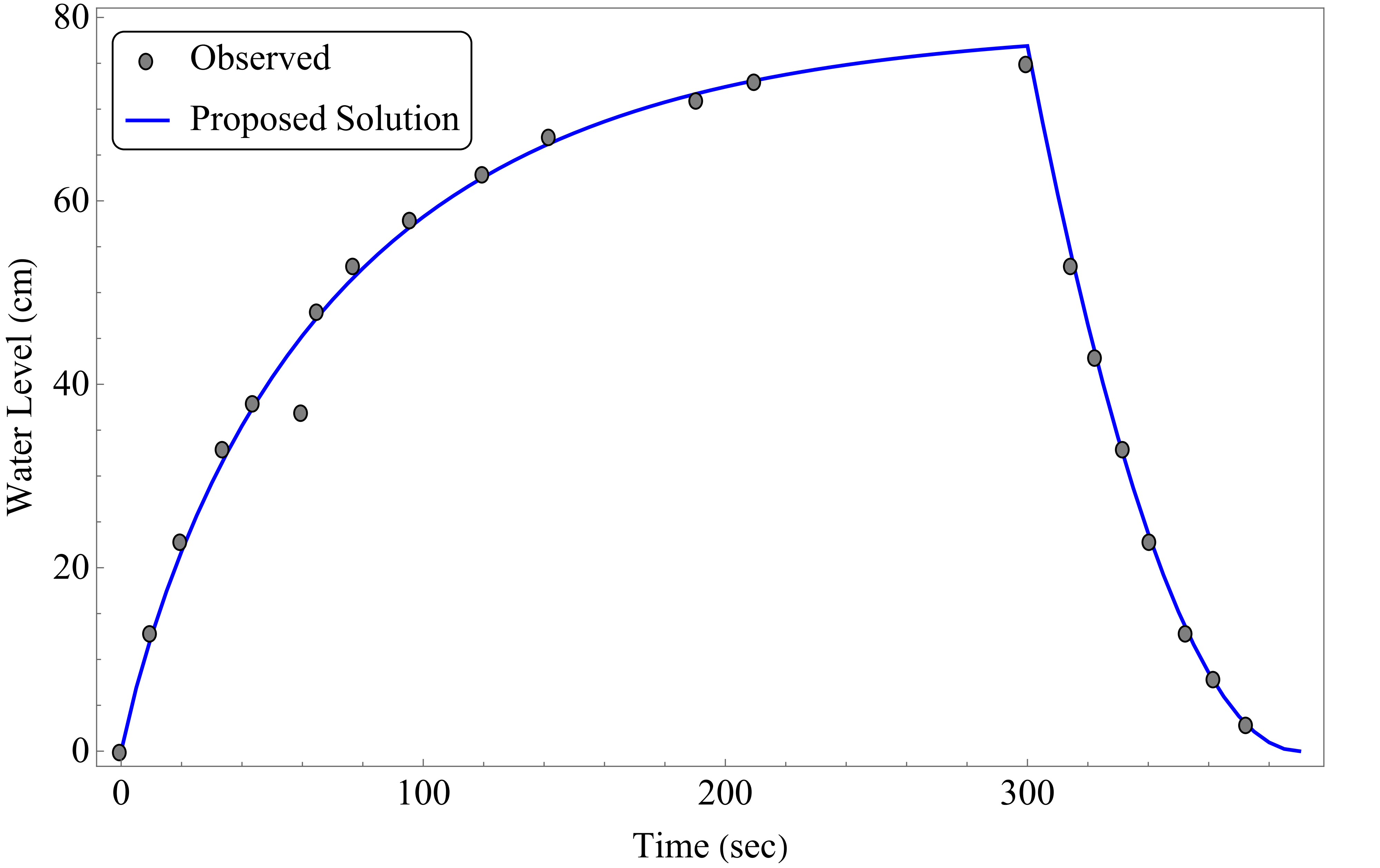

Observed
Proposed Solution
Water Level (cm)
Time (sec)
0
20
40
60
80
0
100
200
300

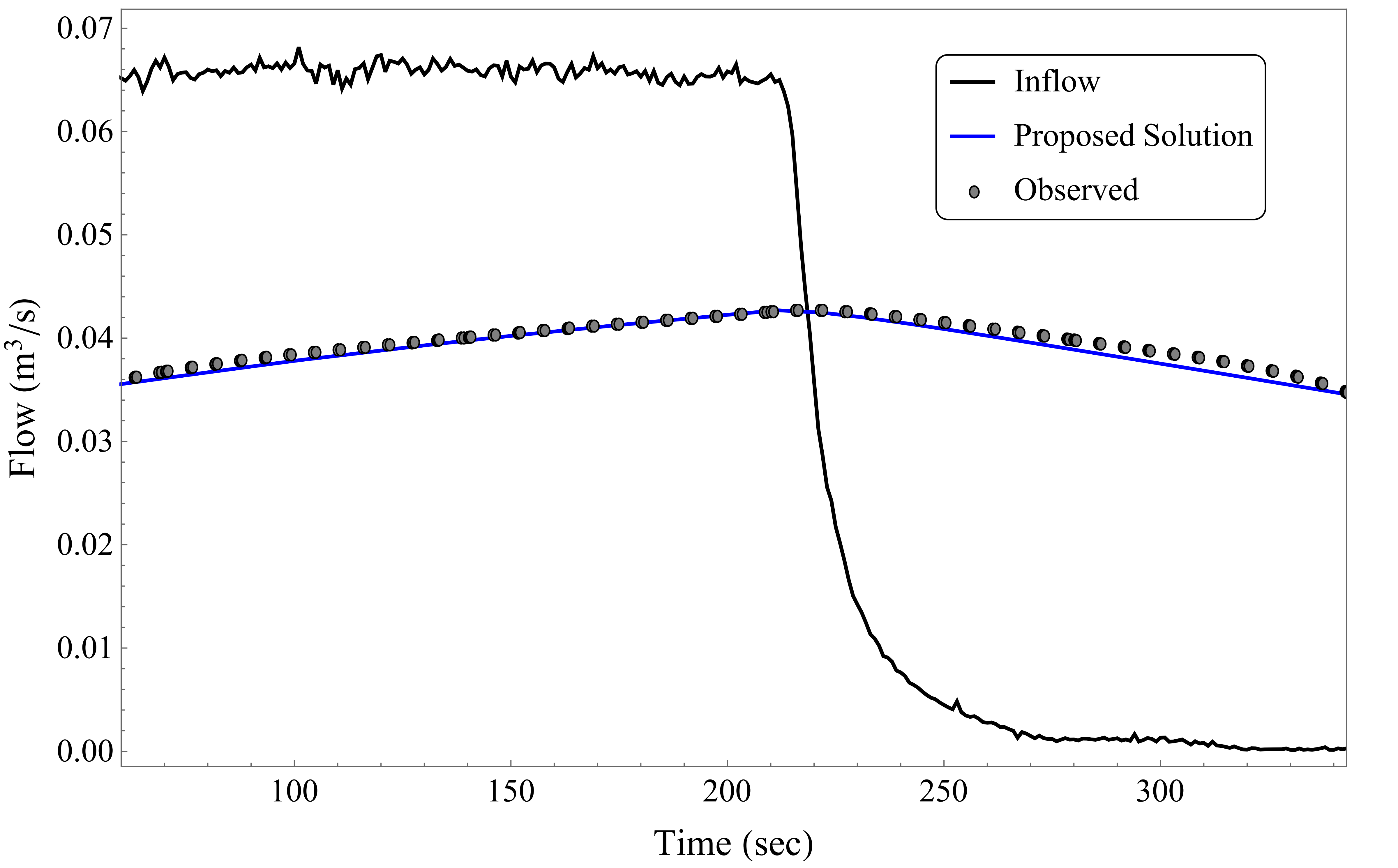
Inflow
Proposed Solution
Observed
Flow (m^3/s)
Time (sec)
0.00
0.01
0.02
0.03
0.04
0.05
0.06
0.07
100
150
200
250
300

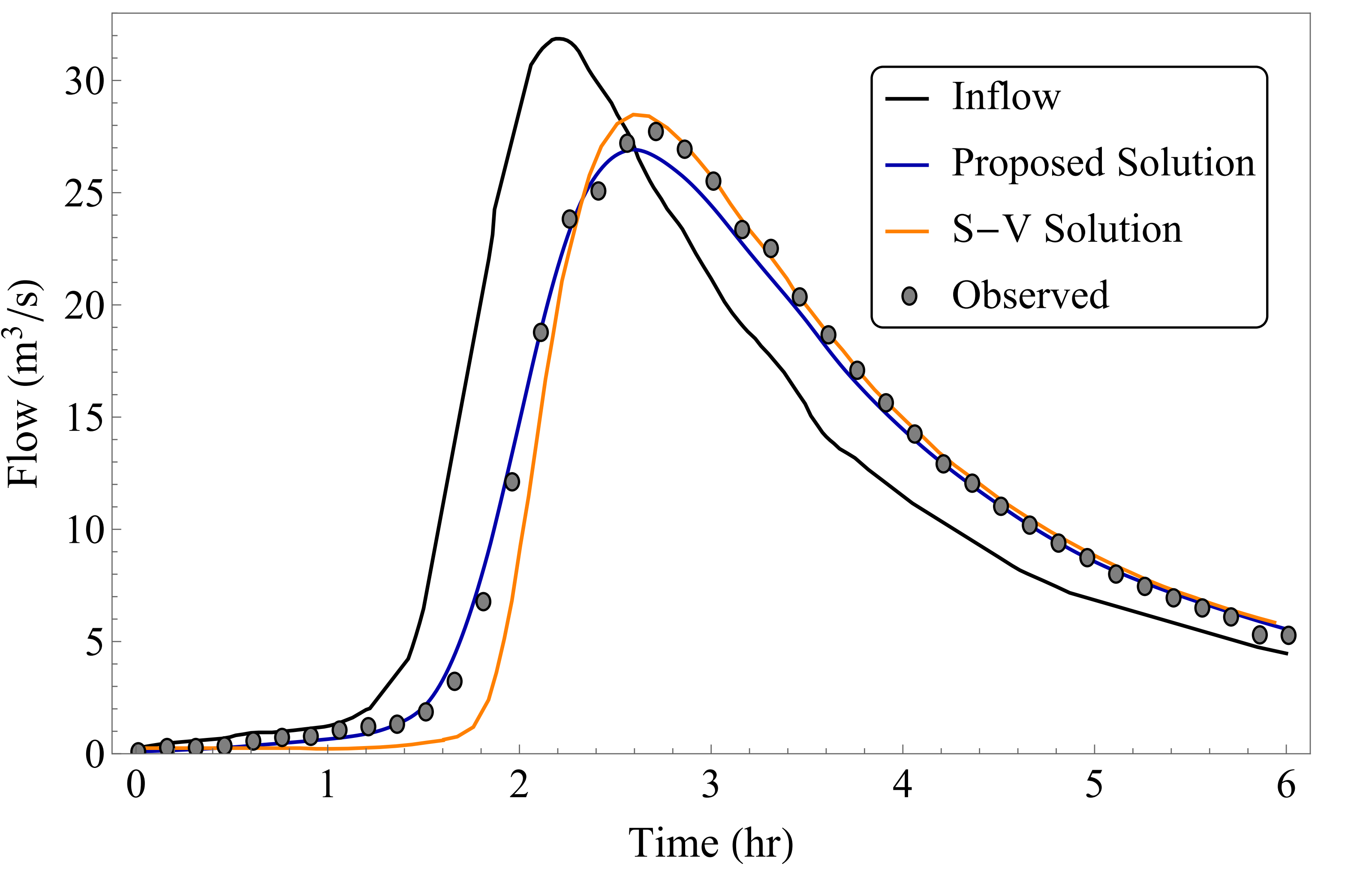

Inflow
Proposed Solution
S−V Solution
Observed
Flow (m^3/s)
Time (hr)
0
5
10
15
20
25
30
0
1
2
3
4
5
6

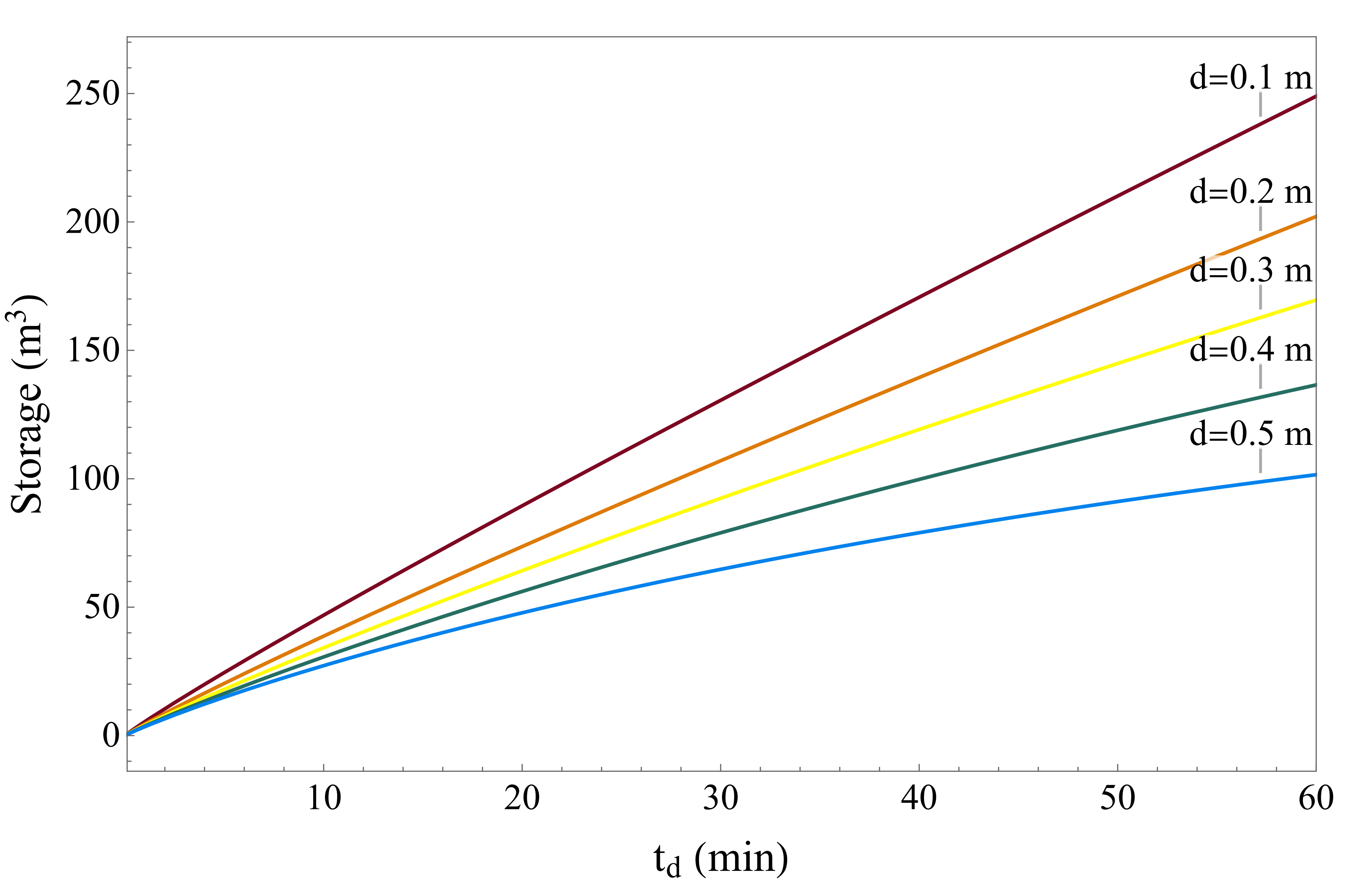

d=0.1 m
d=0.2 m
d=0.3 m
d=0.4 m
d=0.5 m
Storage (m³)
250
200
150
100
50
0
10
20
30
40
50
60
t_d (min)

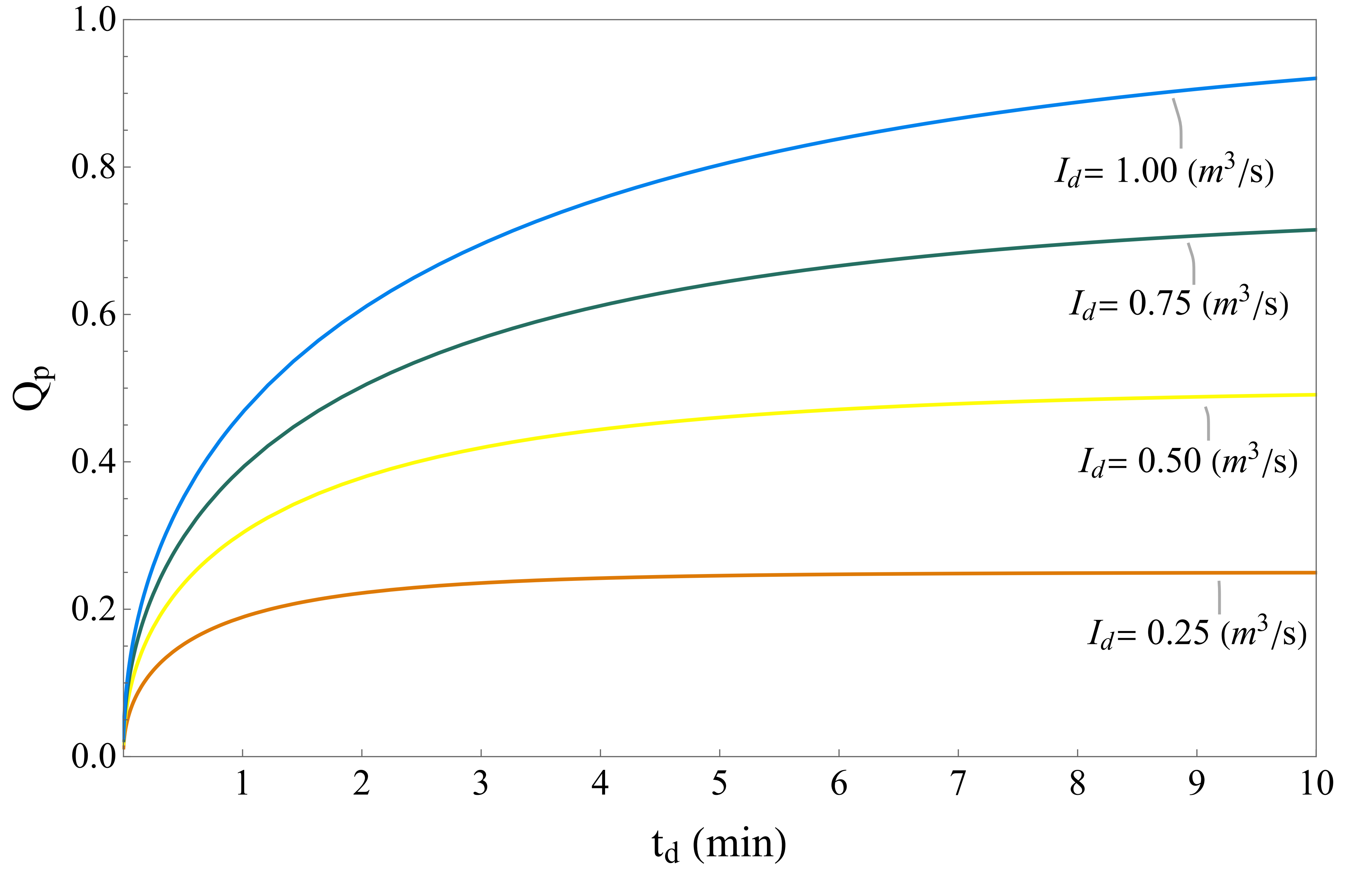
1.0
0.8
0.6
0.4
0.2
0.0
1
2
3
4
5
6
7
8
9
10
Q_p
t_d (min)
I_d= 1.00 (m^3/s)
I_d= 0.75 (m^3/s)
I_d= 0.50 (m^3/s)
I_d= 0.25 (m^3/s)

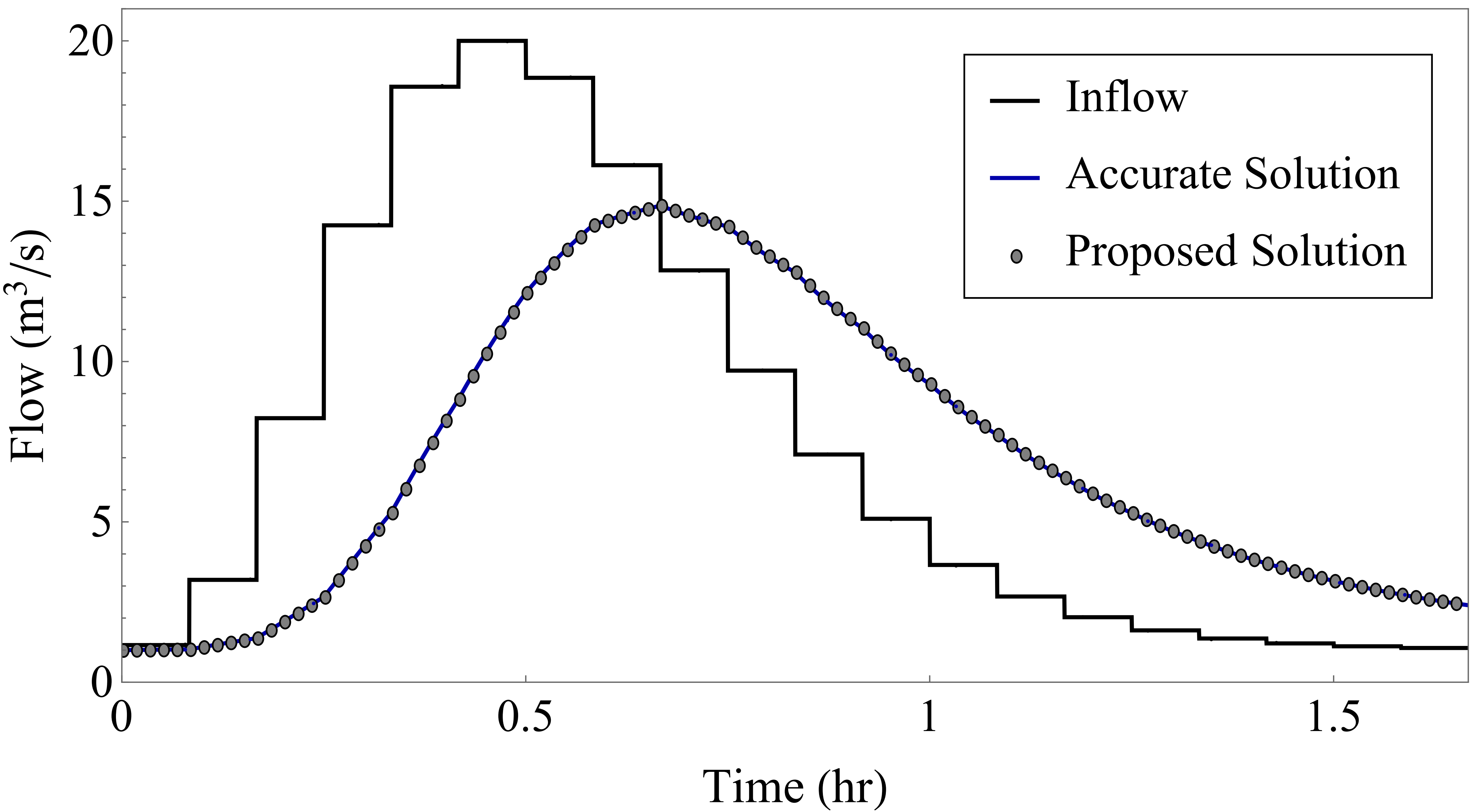

Inflow
Accurate Solution
Proposed Solution
Flow (m3/s)
Time (hr)
0
5
10
15
20
0
0.5
1
1.5